Icarus 252 (2015) 95–106

Contents lists available at ScienceDirect

Icarus

journal homepage: www.elsevier.com/locate/icarus

Small-scale lunar graben: Distribution, dimensions, and formation processes

Renee A. French [a,*], Craig R. Bina [a], Mark S. Robinson [b], Thomas R. Watters [c]

[a] Northwestern University, Department of Earth and Planetary Sciences, 2145 Sheridan Rd, Evanston, IL 60208-3130, USA
[b] Arizona State University, School of Earth and Space Exploration, Tempe, AZ 85287, USA
[c] Smithsonian Institute, National Air and Space Museum, Center for Earth and Planetary Studies, Washington, DC 20013, USA

ARTICLE INFO

Article history:
Received 14 August 2014
Revised 4 November 2014
Accepted 28 December 2014
Available online 10 January 2015

Keywords:
Moon
Tectonics
Moon, surface
Geological processes

ABSTRACT

The Lunar Reconnaissance Orbiter Camera (LROC) is the first instrument to provide widespread coverage with a range of incidence angles at the resolution required to detect small-scale landforms. A sample (n = 238) of globally distributed, small-scale graben average 26 m wide and 179 m long. When dividing the population into those located within mare and highland regions, we observe that graben located within mare tend to be narrower, shorter, and more irregularly spaced than those in highland terrane. For graben associated with contractional landforms, those in mare are smaller in width and length than those in highlands; the same is true for graben independent of contractional landforms. Assuming a simple geometry, widths of mare graben associated with scarps or ridges are used to estimate the minimum depth range to a mechanical discontinuity (e.g., base of the regolith) resulting in values of ~4–48 m. These values are similar to the ranges estimated for regolith thickness from previous workers using Apollo 14 seismic data (3.9–8.5 m), crater counting techniques (8–33 m), crater morphology techniques (2.5–9 m), and crater blockiness (8–31 m). Widths of highland graben yield minimum depths of faulting of 209–296 m. While this range agrees well with models for regolith production (an older surface will have thicker regolith), this estimate likely does not represent the thickness of a mechanical unit due to the fragmented nature of the highland crust (it does not provide a defining boundary between bedrock and regolith). Spacing of mare graben not associated with contractional landforms is used to estimate maximum local mare unit thickness for two graben groups: 190 m for Posidonius and 296 m for Vitello. Maximum graben ages range from late Eratosthenian to early Copernican based on superposed and crosscut crater ages with a group of graben deforming ejecta from Copernicus crater. Data presented here provide further evidence of a globally distributed, young, small-scale graben population that has formed as a result of localized extension either from flexural bending or dilation due to contractional faulting or volcanic uplift, indicating a significant level of recent geologic activity.

1. Introduction

Large-scale linear and arcuate rilles or graben and contractional wrinkle ridges on the Moon were first reported within and around mare basins (Gilbert, 1893; Arthur, 1962). The formation and spatial distribution of these tectonic features is attributed to basin-localized stresses related to load-induced flexure and subsidence (Maxwell et al., 1975; Wilhelms, 1987). Presently, the Lunar Reconnaissance Orbiter Camera (LROC) is providing unprecedented coverage of the lunar surface, with Narrow Angle Camera (NAC) image pixel scales of 0.5–2 m, and Wide Angle Camera (WAC) image pixel scales of 100–400 m (Robinson et al., 2010). The meter-scale pixels and range of incidence angles (~30–80°) are necessary to identify and characterize small tectonic features. Such features include lobate scarps, defined as linear to arcuate surface expressions of low-angle thrust faults (Howard and Muehlberger, 1973; Binder and Gunga, 1985; Watters and Johnson, 2010; Watters et al., 2010) with lengths of hundreds of meters to kilometers (Banks et al., 2012). Other such features are graben, characterized by narrow, flat-floored depressions with lengths that exceed widths and bounded by two steeply dipping antithetic normal faults (e.g., Golombek, 1979; McGill and Stromquist, 1979). Typical dimensions of small-scale graben range from tens to hundreds of meters wide and up to a couple kilometers in length, making these a distinct population from the basin-related graben.

* Corresponding author.
E-mail address: renee@earth.northwestern.edu (R.A. French).

http://dx.doi.org/10.1016/j.icarus.2014.12.031
0019-1035/

Small-scale graben were noted by Watters et al. (2010) in association with the Lee-Lincoln scarp and are oriented subparallel and perpendicular to the strike of the scarp. The formation of these graben was interpreted as a result of regolith and bedrock extension due to flexural bending during formation of the Lee-Lincoln scarp (Watters et al., 2012a). Additional small-scale graben have been discovered, with estimated ages on the order of 50 Ma (Watters et al., 2012a) based on crosscutting relationships with small-diameter impact craters, lack of superposed craters, and infilling rates of shallow depressions, indicating recent extension on a body that is globally contracting.

Lunar Orbiter Laser Altimeter (LOLA) profiles (Smith et al., 2010) of Vitello graben show that they occur along a topographic rise or ridge-crest on the flank of a wrinkle ridge, but it is questionable whether the formation of these graben is connected with tectonic activity related to the ridge (Watters et al., 2012a). If some small-scale graben are not a result of overall contraction and are unrelated to scarp or ridge formation, an alternative hypothesis that involves uplift and flexural bending due to a subsurface laccolith was suggested by Watters et al. (2012a). If this is true, then the apparent young age of the graben would require Copernican-aged intrusive volcanism on the Moon, but previous workers have suggested this activity ceased much earlier (see review by Shearer et al., 2006). However, localized Copernican-aged extrusive volcanism, such as the Ina-D feature, has been discovered (Schultz et al., 2006; Braden et al., 2014). Crater counts on a newly identified population ($n = 75$) of Ina-style features indicate absolute model ages between 20 and 60 Ma, and equilibrium crater populations suggest ages less than 100 Ma (Braden et al., 2014).

Graben are observed on all of the terrestrial planets and many icy satellites (Schultz et al., 2010; Watters et al., 2010) and are generally larger (hundreds of meters up to tens of kilometers in width; Watters and Schultz, 2010) than the small-scale lunar graben. On Earth, studies have shown that graben form in both extensional and compressional tectonic environments (McGill and Stromquist, 1979; Gordon and Lewis, 1980; Campbell and Bentley, 1981; Philip and Meghraoui, 1983; Schlische et al., 1996) and in association with volcanism (Rubin and Pollard, 1988). On Mercury, graben are almost exclusively confined to the interiors of impact basins and volcanic smooth plains that have buried basins and craters (i.e., ghost craters) (Watters et al., 2009, 2012b; Prockter et al., 2010). Their formation is generally attributed to uplift due to load-induced stresses (basin exterior annular loading), lateral crustal flow, or thermal contraction of thick cooling units (Melosh and McKinnon, 1988; Watters et al., 2005, 2009, 2012b; Kennedy et al., 2008; Head et al., 2009; Freed et al., 2012). Venusian graben along fracture zones may be linked to mantle dynamics (Solomon et al., 1991) or gravitational spreading (Phillips and Hansen, 1994), while graben observed around coronae and chasmata are likely due to load-induced stresses (upwelling or loading of magmatic material) or as dilation over dike intrusions (Hansen and Phillips, 1993; Ernst et al., 2003; Krassilnikov and Head, 2003; Grindrod et al., 2005). Martian graben are thought to originate either as a consequence of tectonic rifting, dilation over dike intrusions, or from load-induced stresses (i.e., Tharsis) (Banerdt et al., 1992; Wilson and Head, 2002; Cailleau et al., 2003; Mège et al., 2003; Schultz et al., 2004; Golombek and Phillips, 2010).

This paper seeks to characterize the spatial distribution and dimensions of small-scale lunar graben. Graben dimensions and spacing are used to provide constraints on depth of faulting and faulted layer thickness. We make comparisons between mare and highlands graben, as well as graben associated and unassociated with lobate scarps or wrinkle ridges, in order to illuminate trends between different groups. Graben age is estimated using the principles of superposition and crosscutting relationships. Finally, we present a few examples of graben likely formed by different mechanisms and relate them to current understanding of recent surface activity on the Moon.

2. Data and methods

Graben were found by searching LROC NAC images, which have 100% coverage from ±60° to ±90° latitude and over 50% coverage from −45° to 45° latitude with incidence angles favorable for morphologic interpretations (45–80°). A random sample from the current population was selected for this study, while ensuring that the sample had a good spatial distribution.

Processing of LROC NAC images (radiometric calibration, map projection, mosaicking) was performed using the United States Geological Survey Integrated Software for Imagers and Spectrometers (ISIS) software package (Anderson et al., 2004). Graben length, maximum width, and spacing were measured directly from NAC images using ISIS. Measurement uncertainties are resolution dependent and vary with the scale of the graben but are conservatively on the order of two pixels, resulting in uncertainties less than 10% for graben lengths and less than 33% for graben widths. A Wide Angle Camera (WAC) 100 m global mosaic (Speyerer et al., 2011) was used for regional coverage.

Lengths and maximum widths of 238 individual graben are measured within 23 groups, where a group is defined as a geographically isolated system of graben. A set of graben represents those with similar orientation within a given group, and a group can have multiple sets of graben. The orientation for each graben is visually estimated with uncertainties of roughly ±5°. Fault segment lengths are measured for faults that grew by en echelon stepping. Only troughs with two observable bounded sides are measured and used for statistical analysis (half graben are not included). Although some graben are found within large impact basins dated Imbrian or older (Losiak et al., 2009), the graben are considered to have formed in the respective unit (mare or highlands) in which the crater is located. For the purposes of clarity and brevity, when we refer to 'graben width' later in the paper, we are describing the maximum graben width.

Topographic data for Posidonius are derived from WAC stereo models (GLD100) and have a mean vertical accuracy of better than 10 m for the nearside maria and better than 20 m over the entire dataset (Scholten et al., 2012). Topographic data for Copernicus were derived from NAC stereo pairs with a precision error of 1.86 m and a root mean square (RMS) error with LOLA elevations (nine different orbital tracks) of 1.35 m. Topography is used to determine if graben are related to the structural relief of the lobate scarp or wrinkle ridge. If topographic data are not available, scarp association is determined by relative location (i.e., in the backscarp terrain) and distance from the scarp face (up to several kilometers). Graben associated with wrinkle ridge formation may be located on the ridge (formed by flexural bending) or along its flanks (formed by dilation). Also, if graben are bounded by ridges and are located within the crossover area between ridge segments, they are considered related to the wrinkle ridge (formed by dilation).

3. Results

3.1. Spatial distribution and orientation

We find small-scale graben distributed globally (Fig. 1), consistently near lobate scarps (in the highlands) and wrinkle ridges (in the maria). However, a couple of groups – Copernicus and Posidonius – are not located within close proximity (~few kilometers) to a scarp or ridge. The Vitello, Virtanen, and Posidonius graben occur along topographic rises that do not appear to be connected to any

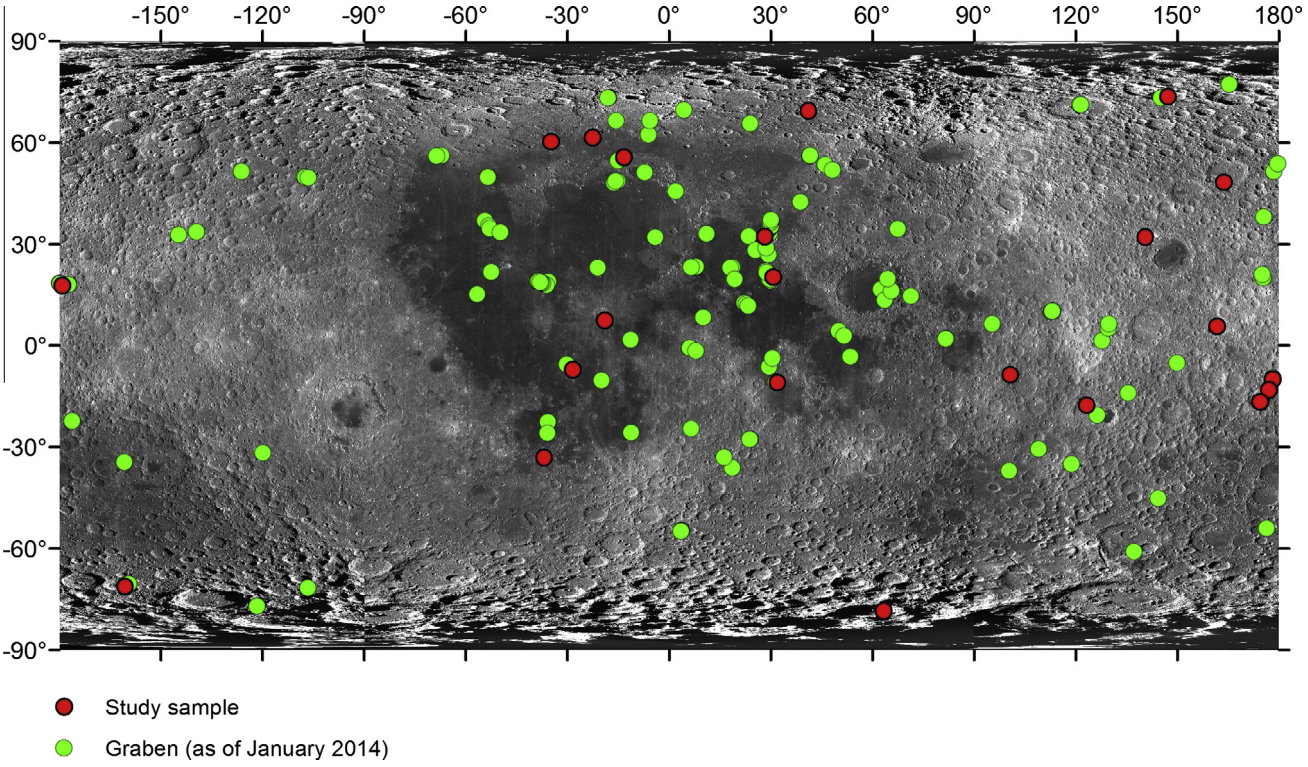

Fig. 1. Distribution of small-scale graben discovered since January 2014 (green dots) and the sample analyzed in this study (red dots). Background is a WAC global monochrome mosaic with a native resolution of 100 m/pixel (Speyerer et al., 2011). (For interpretation of the references to color in this figure legend, the reader is referred to the web version of this article.)

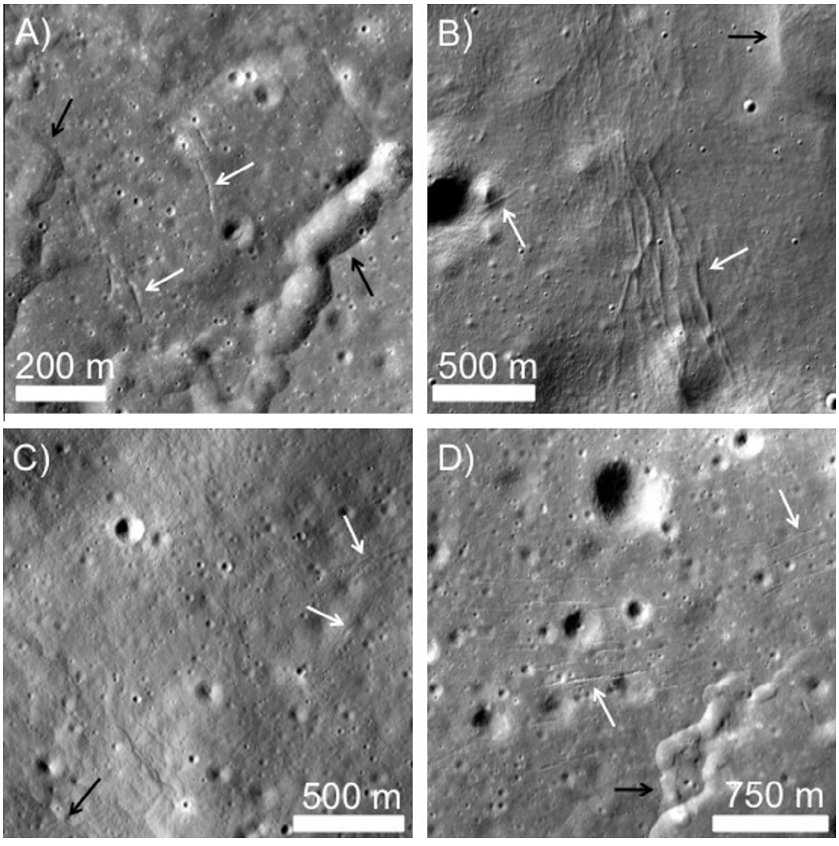

Fig. 2. Examples of small-scale graben, north is up in all images. White arrows point to graben and black arrows point to the nearby scarp or ridge. (A) Aitken graben situated within ~300 m of two wrinkle ridges (LROC NAC frame M105730242RE). (B) Arnold A graben located up to ~4 km southwest of a lobate scarp (LROC NAC frame M159692720RE). (C) Lutke graben formed ~1 km northeast of a lobate scarp (LROC NAC frame M134381673RE). (D) Vitello graben located less than ~1.5 km north of a wrinkle ridge (LROC NAC frame M104756463RE).

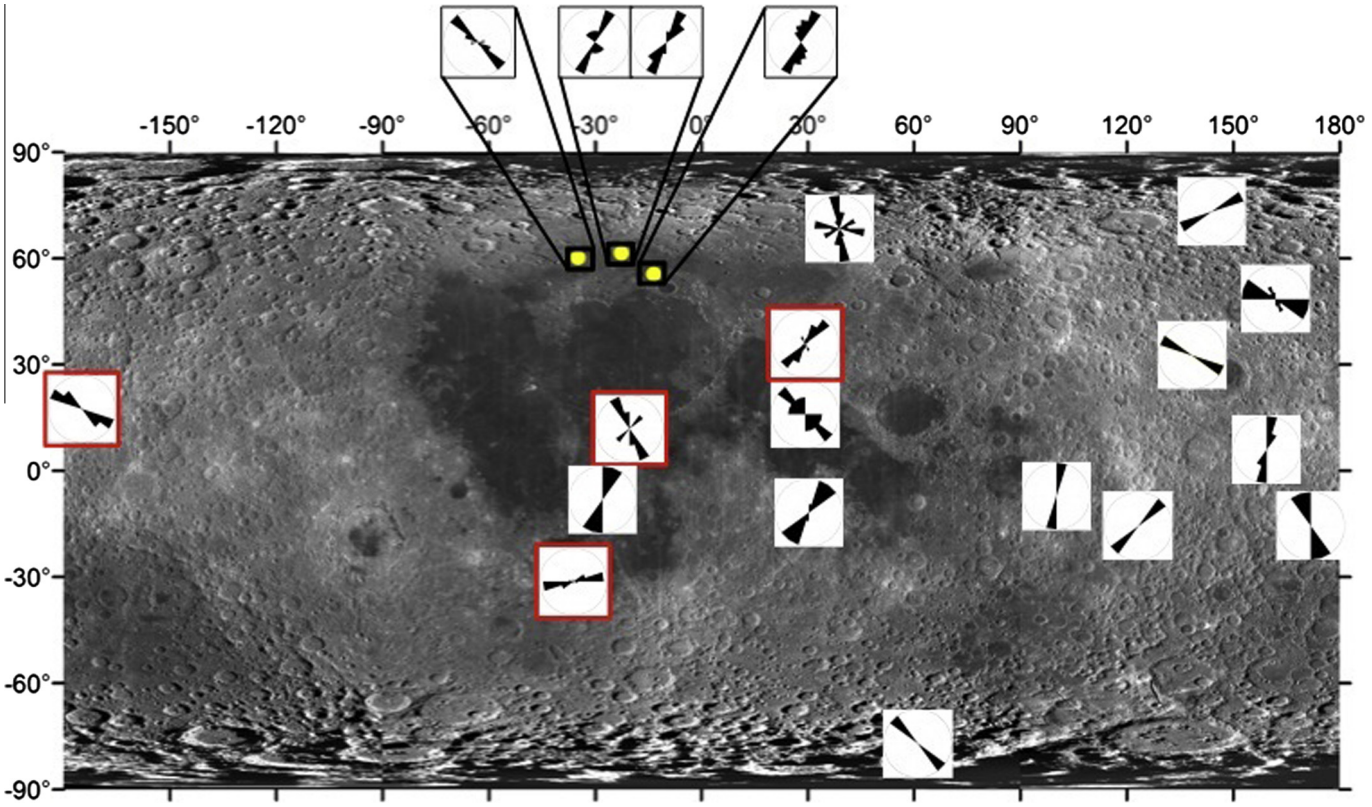

Fig. 3. Orientations of graben sampled for this study. Graben not associated with contractional landforms are outlined in red. Only groups with more than two graben ($n > 2$) are included. (For interpretation of the references to color in this figure legend, the reader is referred to the web version of this article.)

nearby compressional tectonic feature. Aitken, Arnold A, Demonax, D'Alembert, Lutke, Mandel'shtam, Numerov, Posidonius, Racah U, and Seares graben formed within Imbrian or older craters.

Graben orientation with respect to scarps and ridges varies widely, sometimes changing from near perpendicular to near parallel within a single group (Fig. 2). Graben near Aitken crater are located less than 300 m from two wrinkle ridges (Fig. 2A) and are oriented roughly perpendicular to both ridges. The Arnold A graben (Fig. 2B) extend up to ~4 km from a scarp aligned with the rim of a crater and change orientation (parallel to perpendicular) further from the scarp face. Graben are oriented roughly perpendicular to the Lutke lobate scarp (Fig. 2C) and are located ~1 km from the scarp face. The Vitello graben are located less than ~1.5 km from a wrinkle ridge and change orientation from roughly parallel to ~45° to the strike of the ridge (Fig. 2D).

Fig. 3 shows the orientation (from north) of each graben group with $n > 2$. Some graben display consistent orientations with neighboring groups, but others show completely opposite orientations. While the majority of individual graben groups exhibit a preferred or dominant orientation, Arnold A, Copernicus, Plato T, and Posidonius graben have orientations that vary significantly (by as much as ~90°) within each group. When comparing graben orientations with nearby scarps, 23% are within ~20° of the orientation of the related scarp and 26% differ by more than ~70°.

3.2. Width distribution

The distribution of graben width (w; $n = 238$) is shown in Fig. 4 and listed in Table 1, with a mean (μ_w) of 26 m ($\sigma_w = 47$ m), skewness (measure of symmetry, positive is right-skewed) of 5.7, and a sample excess kurtosis (measure of "peakedness") of 36.0. The median (M) width is 15 m, consistent with a right-skewed distribution due to the larger Copernicus, Numerov, and Virtanen graben

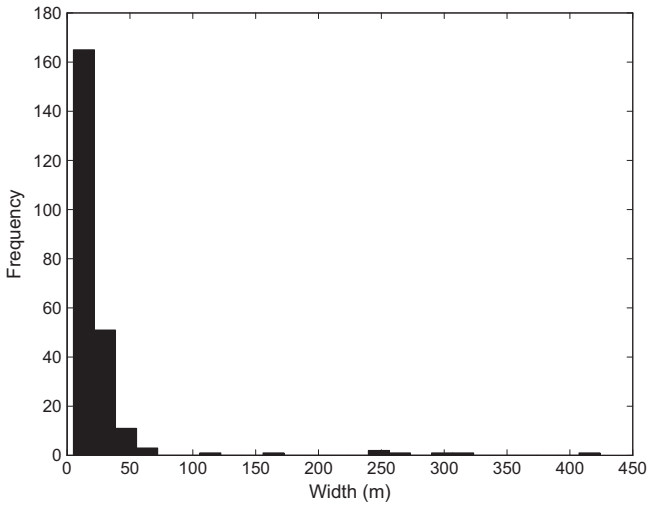

Fig. 4. Distribution of graben width: $\mu_w = 26$ m, $\sigma_w = 47$ m, $M_w = 15$ m, skewness is 5.7, and sample excess kurtosis is 36.0.

which range in width from ~45 m to ~425 m. All of the Virtanen graben ($n = 5$) are larger than the rest of the entire population of small-scale graben in our study sample, while the Copernicus and Numerov graben are more variable. If the Copernicus, Numerov, and Virtanen graben are excluded, the mean is 18 m with a standard deviation of 10 m.

3.3. Length distribution

Graben lengths (l; $n = 238$; Fig. 5, Table 1) have a mean (μ_l) of 179 m ($\sigma_l = 204$ m), skewness of 4.2, and sample excess kurtosis

Table 1
Small-scale graben sampled for this study (see Fig. 1 for distribution). Gray rows denote mare graben. M = median, μ = mean, σ = standard deviation.

Lat (N)	Lon (E)	Name	LROC image ID	# of graben	Length (m)	Length $M/\mu/\sigma$ (m)	Max. width (m)	Max. width $M/\mu/\sigma$ (m)	Scarp/wrinkle ridge associated?
−16.64	174.397	Aitken	M105730242RE	4	42–122	84/83/38	40,375	12/12/2005	Y
69.325	41.103	Arnold A	M159692720RE	13	129–700	187/252/178	20–45	33/34/7	Y
7.512	340.908	Copernicus	M1121365830RE	4	308–712	494/502/166	44–424	114.5/174/173	N
48.268	163.343	D'Alembert	M138838221LE/RE	14	46–390	100.5/118/81	Aug-36	20/20/7	Y
−78.315	63.211	Demonax	M124143297LE/RE	3	236–384	323/314/74	16–45	23/28/15	Y
32.04	140.507	Feoktistov	M151956846LE	3	43–82	58/61/20	40,435	10/12/2003	Y
61.536	337.417	Frigoris-1	M102313809RE	7	103–335	173/184/72	32–56	45/44/8	Y
61.484	337.316	Frigoris-2	M127078170LE	6	25–85	38.5/47.5/23	18-Jun	10.5/11.5/5	Y
60.222	325.031	Frigoris-3	M135418485LE/RE	17	27–318	118/128/68	40,351	13/13/5	Y
20.2	30.486	Lee-Lincoln	M104318871LE	6	88–201	155/150/40	Dec-33	24.5/23/7	Y
−17.792	123.284	Lutke	M134381673RE	3	30–198	59/96/90	40,383	38,700	Y
−10.83	31.869	Madler B	M116107010LE	9	54–465	99/140/125	16–41	23/26/8	Y
5.661	161.756	Mandel'shtam	M112896388LE	6	171–411	194.5/248/110	22–36	27.5/28/5	Y
−71.22	199.436	Numerov	M107912831RE	2	251–445	348/348/137	56–115	85.5/85.5/42	Y
−8.664	100.598	Pasteur	M103854211LE	3	165–290	273/242/68	26–38	31/32/6	Y
55.638	346.587	Plato T	M119938550LE/RE	15	27–160	86/89/47	40,314	10/11/2004	Y
32.17	28.23	Posidonius	M124383016LE/RE	63	17–573	90/127/99	40,353	12/12/2005	N
−13.031	177.063	Racah U	M176474587RE	2	67–105	86/86/27	40432.00	35744.00	Y
−10.014	178.099	Racah X-1	M176467785LE	1	112	–	26	–	Y
−7.093	331.53	Riphaeus	M129479105LE	4	25–185	25.5/65/80	28-Jun	14-Oct	Y
74.708	147.152	Seares	M128306716LE	3	157–284	176/206/69	15–41	21/26/14	Y
17.767	180.878	Virtanen	M184704748LE	5	835–1483	1419/1291/268	241–322	263/273/34	N
−33.079	323.073	Vitello	M104756463RE	45	51–522	161/182/101	24-Jul	15/16/4	N

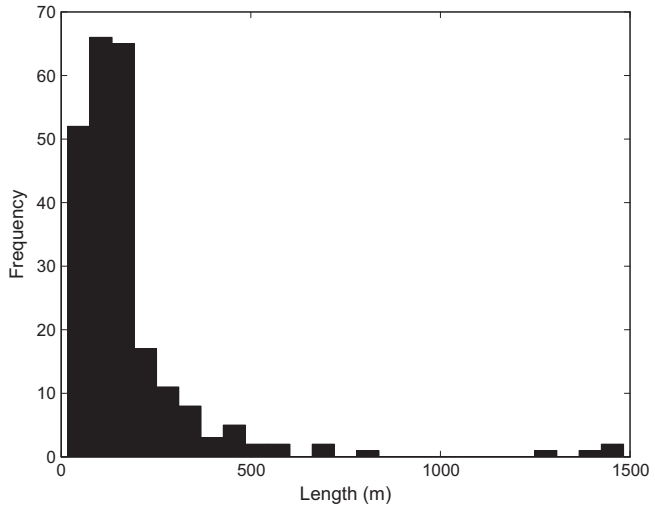

Fig. 5. Distribution of graben length: μ_l = 179 m, σ_l = 204 m, M_l = 136 m, skewness is 4.2, and sample excess kurtosis is 21.5.

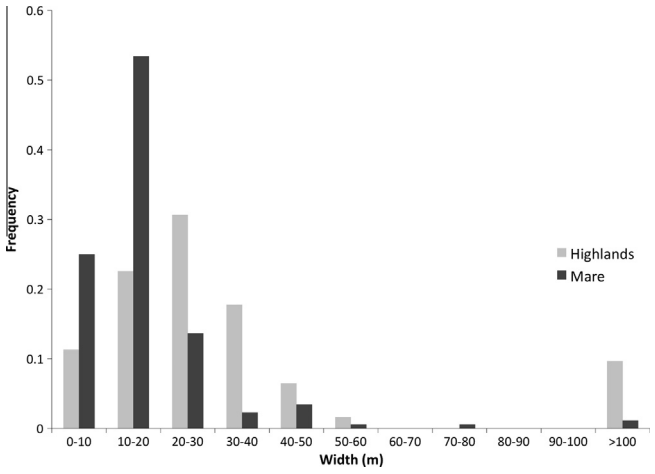

Fig. 6. Distribution of graben widths in mare (n = 176) and highlands (n = 62).

of 21.5. The median (139 m) is smaller than the mean, most likely due to the Copernicus, Numerov, and Virtanen graben, which can be up to an order of magnitude longer than most graben. If these longer graben are excluded, the mean is 147 m with a standard deviation of 106 m.

3.4. Comparison of mare and highland graben dimensions

Distinct differences are observed between graben widths and lengths in mare and highlands regions (Fig. 6, Table 2). In mare, the mean width is 19 m (σ_w = 34 m, M_w = 14 m) and mean length is 146 m (σ_l = 111 m, M_l = 121 m). If Copernicus graben are excluded, the mean width is 15 m (σ_w = 8 m, M_w = 14 m) and mean length is 138 m (σ_l = 96 m, M_l = 120 m). In contrast, mean graben width in the highlands is 50 m (σ_w = 72 m, M_w = 25 m) and mean length is 256 m (σ_l = 305 m, M_l = 167 m). Excluding larger highland graben (Numerov and Virtanen) yields a mean width of 21 m (σ_w = 10 m, M_w = 23 m) and mean length of 187 m (σ_l = 132 m, M_l = 145 m).

Graben dimensions can be further separated into those associated and not associated with contractional landforms (i.e., lobate scarps and wrinkle ridges) for both mare and highlands (Table 2). Lengths and widths of mare graben associated with scarps or ridges average 117 m (σ_l = 78 m, M_l = 103 m) and 19 m (σ_w = 12 m, M_w = 15 m) respectively, while those independent of scarps or ridges average 162 m (σ_l = 124 m, M_l = 142 m) and 19 m (σ_w = 42 m, M_w = 13 m). For the highlands, lengths and widths of graben that are associated with scarps average 184 m

Table 2
Dimensions for mare and highlands graben. All values are in meters.

	Mare	Highlands	Scarp/ridge-associated (mare)	Scarp/ridge-associated (highlands)	Scarp/ridge independent (mare)	Scarp/ridge independent (highlands)
Average length	146	273	117	184	162	1291
Median length	121	167	103	154	142	1419
Standard deviation	111	337	78	133	124	268
Average width	19	46	19	26	19	273
Median width	14	25	15	24	13	263
Standard deviation	34	70	12	16	42	34

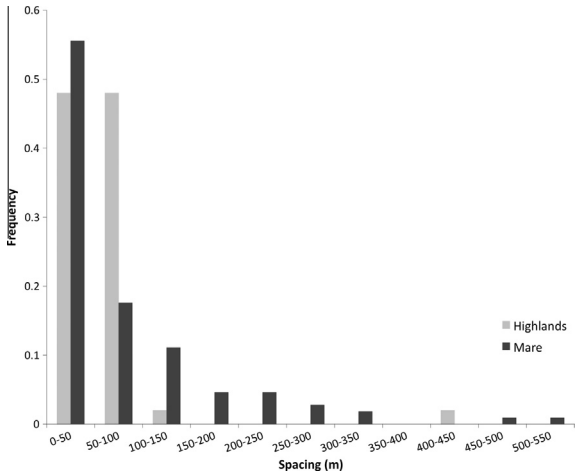

Fig. 7. Distribution of graben spacing in mare ($n = 108$) and highlands ($n = 50$).

($\sigma_l = 133$ m, $M_l = 154$ m) and 26 m ($\sigma_w = 16$ m, $M_w = 24$ m), respectively, and graben independent of scarps (only the Virtanen graben for this sample study) average 1291 m ($\sigma_l = 268$ m, $M_l = 1419$ m) and 273 m ($\sigma_w = 34$ m, $M_w = 263$ m).

3.5. Spacing

Mean spacing between individual graben ($n = 158$) was measured for 15 groups with a mean of 76 m ($\sigma_s = 86$ m). However, when these measurements are separated into mare and highlands components, distinct differences are observed (Fig. 7, Table 3). For mare graben ($n = 108$), 88% are within one standard deviation ($\sigma_m = 95$ m) of the mare mean ($s_m = 83$ m). Two mare graben groups, Vitello and Posidonius, have greater average spacing and are not believed to be associated with a scarp or wrinkle ridge. If these groups are removed from the mare statistics, the resulting mean and standard deviation are 36 m and 25 m, respectively. In contrast, 96% of highlands graben ($n = 50$) are within one standard deviation ($\sigma_{nm} = 61$ m) of the highlands mean ($s_{nm} = 60$ m). It is important to note that the difference in distribution may be affected by the difference in sample size between the mare ($n = 108$) and highlands ($n = 50$).

4. Discussion

4.1. Mechanical discontinuity and layer thickness estimates

Modeling by Melosh and Williams (1989) suggested that in extensional environments, it is energetically favorable for graben to develop from antithetically dipping normal faults. In this model, fault initiation occurs at the surface and is likely influenced by local inhomogeneities, stress concentrations, or planes of weakness. Graben width is largely dependent on the initiation depth of the normal fault (Melosh and Williams, 1989) and is influenced by the flexural rigidity of the material it forms in, which depends on layer thickness and material properties (e.g., the elastic "stiffness" or Young's modulus) (Buck, 1988; Schultz-Ela and Walsh, 2002; Schultz et al., 2007). The width of a symmetric graben (bounded by antithetic normal faults dipping at ~60°) can approximate layer thickness if the bounding faults converge at the base of the layer (Golombek, 1979). However, since faults likely nucleate at the surface and propagate downward, instead of originating at some discontinuity at depth and propagating toward the surface, graben tend to be asymmetric (Schultz et al., 2007). Thus, the widths of

Table 3
Spacing between graben for different spatial groups.

Graben	Average spacing (m)	Standard deviation (m)	Median spacing (m)	Mare/highlands (M/H)	Scarp/ridge-associated?
Feoktistov	13	4	13	H	Y
D'Alembert	37	22	33	H	Y
Pasteur	50	13	53	H	Y
Seares	50	13	46	H	Y
Racah X-1	61	21	53	H	Y
Arnold A	68	22	72	H	Y
Mandel'shtam	76	9	79	H	Y
Demonax	104	32	104	H	Y
All highland	60	61	52		
Frigoris-3	25	9	25	M	Y
Lee-Lincoln	31	12	37	M	Y
Plato T	34	30	20	M	Y
Madler	46	10	47	M	Y
Frigoris-1	70	50	70	M	Y
Posidonius	90	128	39	M	N
Vitello	141	59	139	M	N
All mare	83	95	46		

graben provide a means to estimate a minimum depth of faulting. For the Moon, we make the assumption that antithetic normal faults originating at the surface and propagating downward will encounter a mechanical discontinuity (e.g., regolith, basalt layers) that will hinder their propagation. Therefore, the minimum depth to the mechanical discontinuity can be estimated by $T = 0.5w \times \tan(\theta)$ assuming a simple graben geometry, where T is layer thickness, w is graben width, and θ is fault angle (60° for simple graben) (Golombek, 1979).

Width measurements for mare graben associated with scarps and ridges range from 5 to 56 m, yielding minimum layer thickness estimates of ~4–48 m. These values are similar to the ranges estimated for regolith thickness from Apollo 14 seismic data (3.9–8.5 m; Watkins and Kovach, 1972), crater counting techniques (8–33 m; Wilcox et al., 2005), crater morphology techniques (2.5–9 m; Quaide and Oberbeck, 1968), and crater blockiness (8–31 m; Wilcox et al., 2005). Mare graben independent of scarps and ridges have widths ranging from 6 to 424 m, resulting in minimum layer thickness estimates of 5–367 m. The difference between thickness estimates is likely a function of setting: flexure and dilation associated with scarp and ridge formation only deform the uppermost regolith layer, whereas graben not associated with scarps and ridges are not necessarily confined to near-surface layers.

Widths of highland graben associated with scarps range from 7 to 115 m, resulting in a minimum depth of faulting range of ~6–100 m. For highlands graben independent of scarps (Virtanen graben in this study sample), widths range from 241 to 342 m, yielding minimum depths of faulting of 209–296 m. These greater fault-depth estimates agree well with the idea of greater regolith production: regolith thickness increases with increasing surface age and crater frequency (Shoemaker et al., 1969). However, the idea of regolith "thickness" in the highlands is problematic due to fragmented highland crust overlain by crater ejecta deposits, providing no real defining boundary between bedrock and regolith (Cintala and McBride, 1995).

Graben spacing is a consequence of stress reduction around a fault, which is dependent on the ability of the material to accommodate the stress and strain associated with fault formation (Melosh and Williams, 1989; Ackermann and Schlische, 1997; Cowie and Roberts, 2001). Studies have shown that fault and fracture spacing is dependent on mechanical layer thickness (Bai and Pollard, 2000; Ackermann et al., 2001; Soliva and Benedicto, 2005; Soliva et al., 2006) and material property contrasts, in particular the Young's modulus (Bürgmann et al., 1994; Bonafede and Rivalta, 1999; Bai and Pollard, 2000) which is influenced by layering. Additionally, spacing between faults becomes more regular as the population density increases (Ackermann et al., 2001).

Spacing of mare graben (which are likely bounded) may provide insight into the stress reduction (or stress shadowing) around faults, revealing additional information about thickness of mare basalt sequences. Recent studies have observed thinly layered lava flows in some mare on the order of 10 m thick (Robinson et al., 2012; Enns and Robinson, 2013), possibly interbedded with ash or regolith. There are likely many mechanical layers in mare basalt sequences separated by relatively thin interbeds. However, these interbeds may be too thin to act as mechanical layer boundaries for the normal faults (the faults would effectively ignore them during propagation). Mare sequences with varying interbed thickness may contribute to the slightly larger variation in mare graben spacing (ranging from 5 to 550 m) than highlands graben spacing (ranging from 8 to 443 m) (Fig. 7). Other factors that may contribute to this variation are the range of surface ages, local thickness variation, and material properties that affect how rocks respond to stress and strain. Additionally, inhomogeneities (e.g., buried ejecta blocks, craters) produce a non-uniform deformation field around the faulted rock, affecting the stress-reduction shadow and thus graben spacing.

Graben associated with contractional features likely only deform the uppermost regolith layer, thus spacing of these graben will only reflect regolith thickness. On the other hand, mare graben not associated with contractional landforms do not necessarily deform just an uppermost layer and are more likely to represent confinement in a mechanical layer, thus providing an estimate of local mare unit thickness. For faults confined to a mechanical layer, the equation $s = 0.45T^{1.01}$ can be used to estimate thickness of the layer (here a mare basalt unit), where s is mean spacing and T is thickness (Soliva et al., 2006). Data for two groups, Posidonius and Vitello, show evidence for not being associated with contractional landforms. Spacing between Posidonius graben ranges from 11 to 550 m and averages 90 m, resulting in a mean unit thickness of 190 m. Spacing of Vitello graben ranges from 38 to 283 m and averages 141 m, yielding a mean mare unit thickness of 296 m. Watters et al. (2012a) estimated a minimum mechanical unit thickness of ~80 m for the Vitello graben based on the maximum relief of the topographic rise the graben are found on. Our mechanical unit thickness estimate of 296 m for the Vitello graben is almost four times larger than the value calculated by Watters et al. (2012a), likely due to the relatively low density of faults within graben groups (in addition to the factors listed above). This method of calculating layer thickness using graben spacing may only provide a maximum thickness.

4.2. Formation processes and age estimation

Widths of the Copernicus, Numerov, and Virtanen graben range from ~45 m to 425 m, up to ~1.5 orders of magnitude larger than the rest of the population described in this study. These large widths indicate that the bounding normal faults of the graben are likely not confined to an upper regolith layer. Additionally, the Copernicus and Virtanen graben do not appear to be directly associated with contractional tectonic landforms, indicating a different tectonic setting or formation mechanism (discussed below) than the other graben groups.

Small-scale graben resulting from broad, regional-scale extension are not observed, likely because the Moon appears to be in a general state of global contraction (Solomon, 1977; Binder and Gunga, 1985; Watters et al., 2010, 2012a). Graben that form from localized tension due to scarp or wrinkle ridge formation are commonly observed in this study sample (Fig. 8). Plato T graben (Fig. 8A) are located along the southern edge of Mare Frigoris approximately 8 km from a mare-highland boundary. They occur in the area between an en echelon step of wrinkle ridge segments, are perpendicular to the orientation of the ridges, and likely formed from dilation of the regolith as a result of slip on the wrinkle ridge thrust faults. In contrast, extension observed along the Racah X-1 scarp segment (Fig. 8B) in the highlands is roughly 700 m from and parallel to the scarp face in the back-scarp area, suggesting formation by extensional stresses induced by flexural bending. Two sets of graben are observed along Frigoris-3 (Fig. 8C), located along the northern border of Mare Frigoris approximately 8 km from the mare-highlands boundary. The first set is oriented roughly perpendicular to a wrinkle ridge and exhibits pit chain morphology further from the ridge. In general, pit chains are observed throughout the Solar System and form by material that collapsed into a subsurface void created either by extension from faulting or explosive eruption (Wyrick et al., 2004). Evidence of explosive volcanism around Frigoris-3 graben is absent, so the pit chains likely formed by material collapse during graben formation. The second set of Frigoris-3 graben is located in and perpendicular to an en echelon step of wrinkle ridge segments, suggestive of the same formation mechanism as the Plato

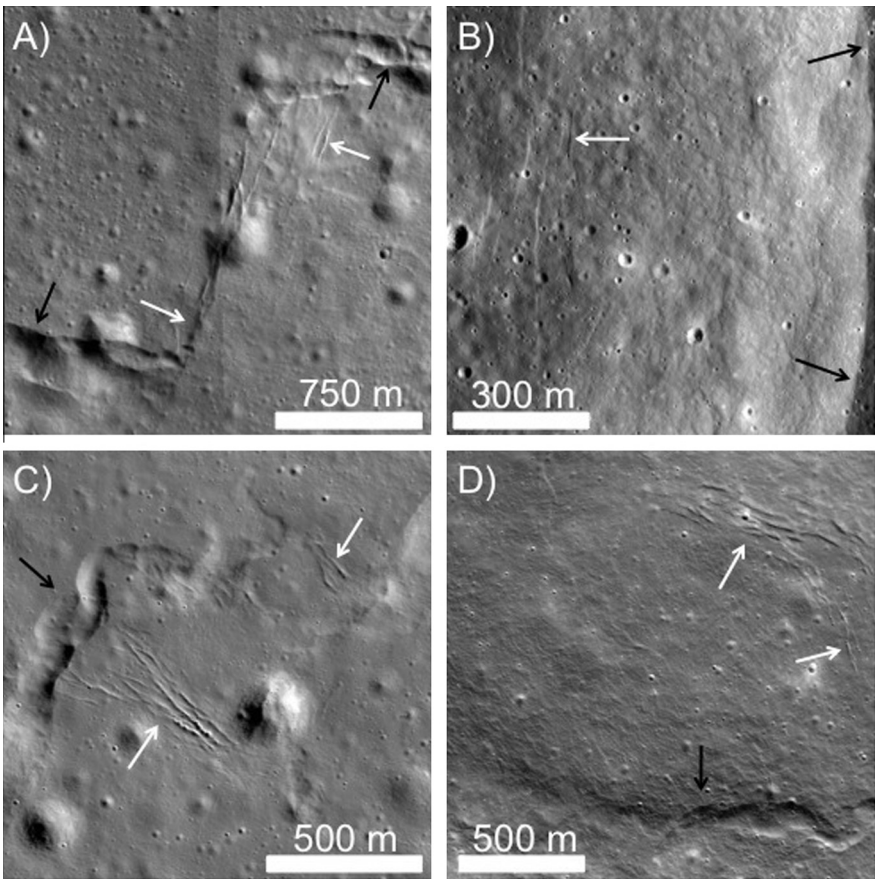

Fig. 8. Examples of graben likely formed through localized tension due to scarp or wrinkle ridge formation. In all images, white arrows point to graben and black arrows point to the lobate scarp or wrinkle ridge. (A) Plato T graben (LROC NAC frames M119938550LE/RE). (B) Racah X1 graben (LROC NAC frame M176467785LE). (C) Frigoris-3 graben (LROC NAC frame M135418485RE). (D) D'Alembert graben (LROC NAC frame M138838221RE).

T graben in Fig. 8A. D'Alembert graben (Fig. 8D) are located along the southern collapsed wall of the D'Alembert impact crater and are coincident with a larger fault complex that spans roughly 125 km in length. The D'Alembert graben occur roughly 1 km from a wrinkle ridge and are oriented parallel to it but then change to sub-perpendicular roughly 650 m from the ridge where the ridge narrows. This reorientation is suggestive of a complex dilation effect caused by the growth of the wrinkle ridge.

Volcanic origins for the extensional stresses that formed small-scale graben are more difficult to discern. The lack of widespread young volcanic flows on the lunar surface – especially near small-scale graben – suggests that extension formed by thermal contraction of mare basalt flows is less likely than intrusive volcanism. Graben formed by intrusive volcanism may be a result of extension induced by the emplacement of laccoliths or dikes (Watters et al., 2012a).

Posidonius crater, a floor-fractured crater (FFC; Schultz, 1976) located on the eastern rim of the Serenitatis basin (Fig. 9), contains small-scale graben (much smaller than the fractures, which are ~500 m to ~2 km wide and up to ~50 km long) far from any compressional tectonic feature, indicating they may have formed as a result of intrusive volcanism. Multiple studies (Brennan, 1975; Schultz, 1976; Wichman and Schultz, 1995, 1996; Jozwiak et al., 2012) suggest that the most probable formation mechanism of FFCs is through shallow magmatic intrusion. The occurrence of small-scale graben in an arcuate pattern that follows the crest of a local topographic high in Posidonius (Fig. 9B and C) suggests formation by uplift from a magmatic intrusion associated with FFC formation. These graben crosscut partially degraded small-diameter (~80–200 m) craters, placing a maximum age between late Eratosthenian and early Copernican (Trask, 1971). Graben exhibit crisp morphology and are not superposed by craters, characteristics indicative of a young age. However, if the graben are related to the topographic rise, the age difference between Posidonius (upper Imbrian; Losiak et al., 2009) and these small-scale graben suggest recent intrusive volcanism connected with or independent of the formation of the FFC.

Pit chains are associated with some small-scale graben in Posidonius and are morphologically similar to those observed with the Vitello graben (Fig. 2D) – which are also found along a topographic rise (Watters et al., 2012a) – possibly suggesting a similar formation mechanism between the two groups. Since evidence of extrusive volcanism has not been observed around these pits, they most likely formed as material collapsed into a subsurface void during graben formation.

Small-scale graben observed roughly 22 km southeast of the rim of Copernicus crater occur along a topographic rise interpreted as part of the Copernicus ejecta blanket (Fig. 10A–C). These graben exhibit complex linkages such as en echelon steps, similar to the Virtanen graben, with steeply dipping walls (Fig. 10D). Lengths reach up to ~700 m, widths up to ~400 m, and depths up to ~12 m with a northwest–southeast orientation. As in the case of the mare graben, the widths can help constrain the local thickness of the Copernicus ejecta blanket. If the graben are confined to the ejecta blanket, a maximum width of 400 m results in a layer thickness of ~350 m (see Section 4.1). This value agrees well with ejecta thicknesses calculated using equations 9 (t = 368 m) and 12 (t = 455 m) from Pike (1974). The similar dimensions and

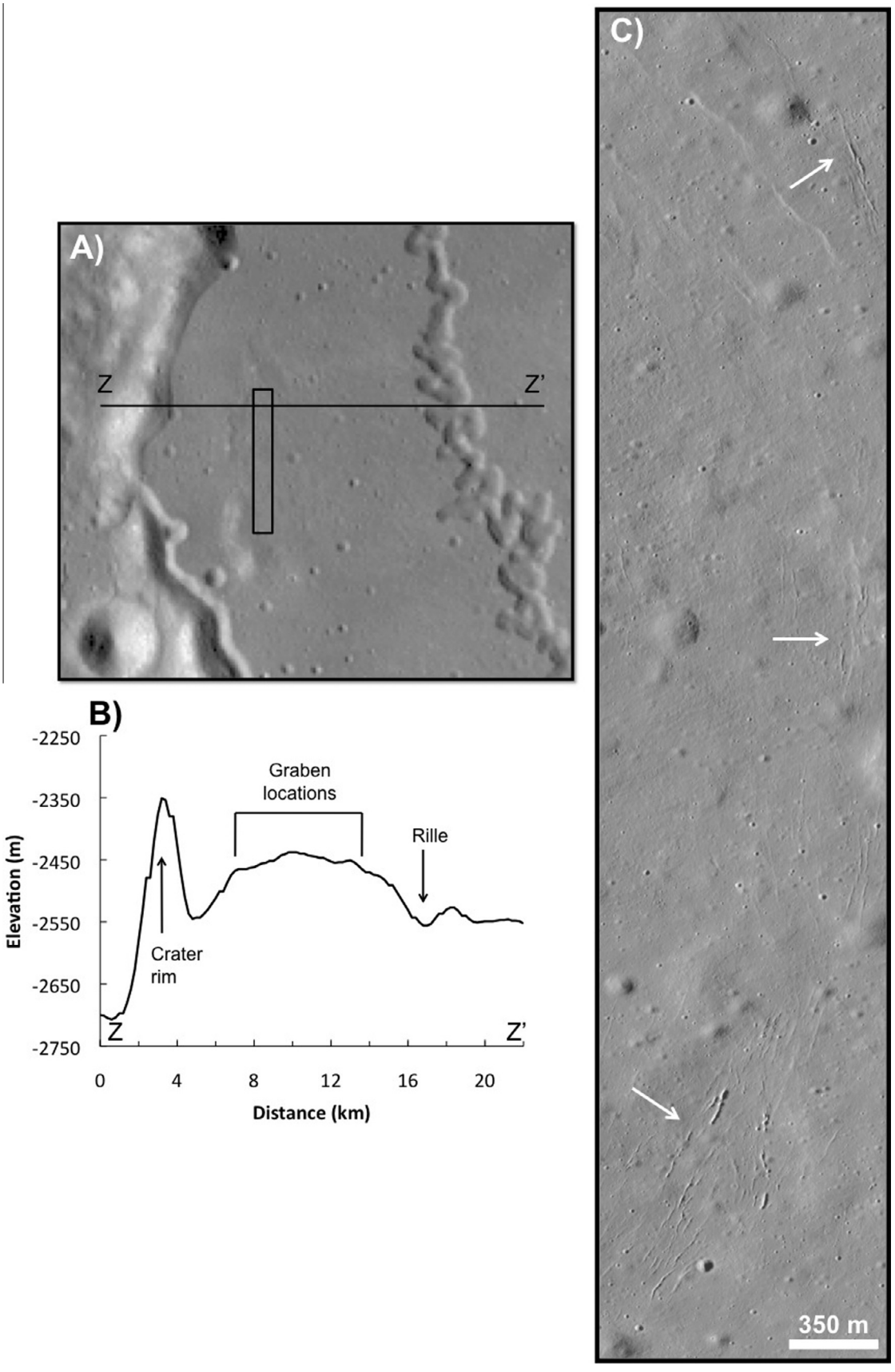

Fig. 9. (A) Western portion of Posidonius crater (LROC WAC monochrome mosaic at 100 m/pixel native resolution). (B) Topographic profile Z–Z′ from (A) using LROC GLD100. Note that graben are located along the domal topographic high (vertical exaggeration ~32:1). (C) Inset from (A) showing arcuate pattern of graben (white arrows, LROC NAC frame M124383016RE).

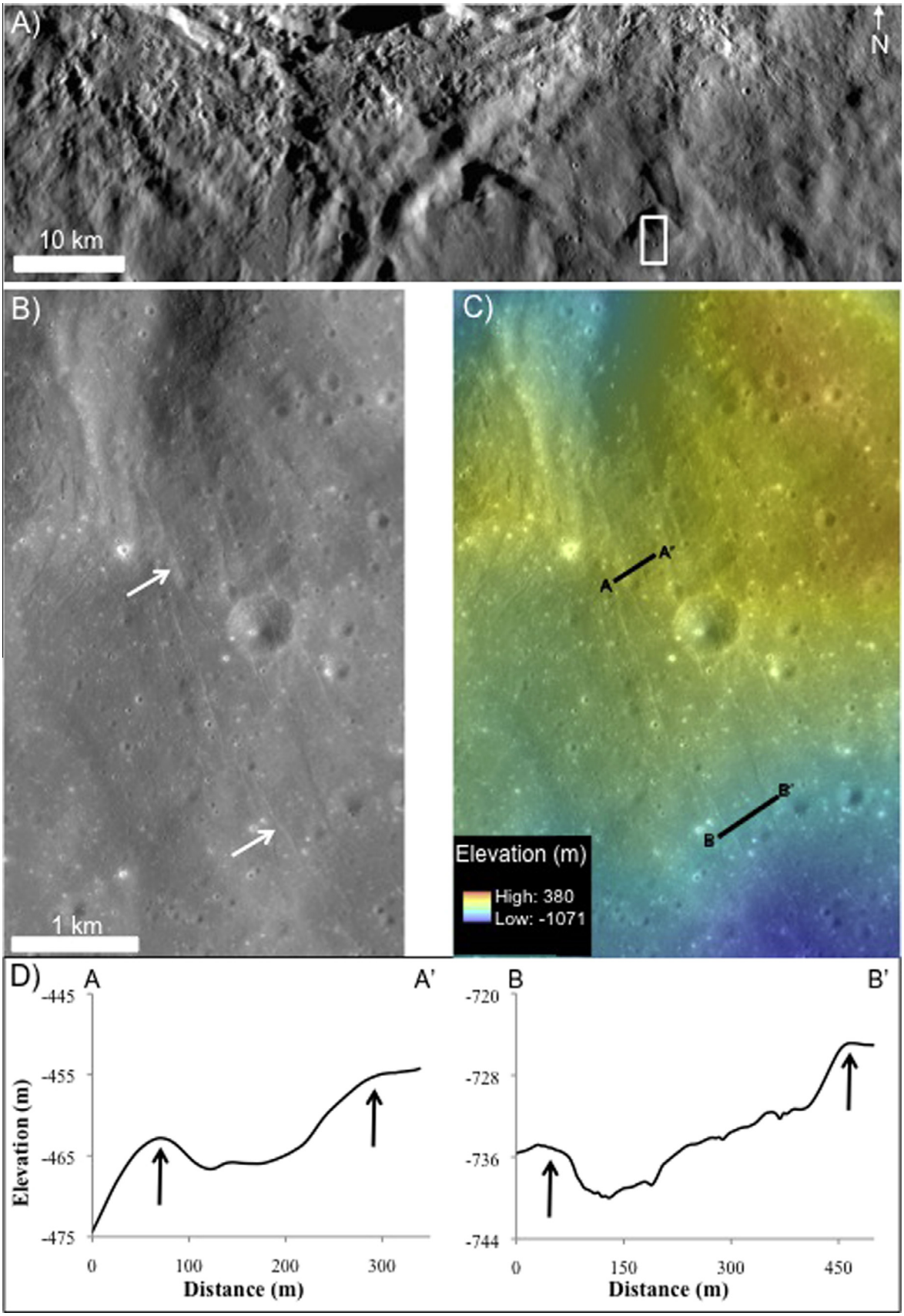

Fig. 10. (A) Graben located roughly 22 km southeast of Copernicus crater (LROC WAC monochrome mosaic at 100 m/pixel native resolution). Sunlight is from the east. (B) Inset from (A), LROC NAC frame M1121365730RE. The white arrows point to graben. (C) Elevation data for the target graben in (B). (D) Topographic profiles A–A′ (vertical exaggeration ~9:1) and B–B′ (vertical exaggeration ~24:1) from (C). Black arrows point to graben rims. Elevations are referenced to a sphere of 1,737,400 m with an accuracy of 1.35 m.

morphology to the Virtanen graben, as well as distance from compressional tectonic features, suggest a different mode of origin not related to compressional tectonics. One possible formation mechanism is volcanic uplift either from a laccolith or dike that could have been induced by the formation of Copernicus. Regardless of the mode of formation, the graben deform Copernicus ejecta and associated secondary craters, clearly showing that they postdate the formation of Copernicus which places their age at less than 800 ± 15 My (Stöffler and Ryder, 2001).

Ages for remaining graben can be estimated using crater morphology. Trask (1971) estimates that craters less than 100 m in diameter formed in the Copernican, independent of degradation state. Likewise, craters up to 400 m in diameter are Copernican (<800 Ma) to Eratosthenian (800 Ma–3.15 Ga; Stöffler and Ryder, 2001) in age, while craters 400 m to 1 km in diameter could be as old as Imbrian (3.15–3.77 or 3.85 Ga; Stöffler and Ryder, 2001) in age. The maximum diameter of craters that are observed superposed on the sample graben is 43 m, placing the crater age firmly in the Copernican. Graben crosscut craters with diameters up to 1 km, but they most commonly crosscut craters with diameters less than 500 m with crater degradation state suggesting formation in the late Eratosthenian to early Copernican. Over half of the craters crosscut by graben have diameters less than 100 m, indicating these graben are of Copernican age.

5. Conclusion

Until recently, lobate scarps were understood to be the youngest tectonic landforms on the lunar surface. High-resolution data from LROC reveal that small extensional landformsalso are present and globally distributed. The population of small-scale graben described here average 26 m wide and 179 m long with azimuthal orientations that vary widely with location. When dividing the population into those located within mare and highlands regions (regardless of their association with contractional landforms) we observe that graben located within mare tend to be narrower, shorter, and more irregularly spaced than those in the highlands. For graben associated with contractional landforms, those in mare are smaller in width and length than those in highlands; the same is true for graben independent of contractional landforms. Three graben groups – Copernicus, Numerov, and Virtanen – have dimensions up to an order of magnitude larger than the rest of the sampled population. When not including these three groups, the mean graben width is 18 m and the mean length is 147 m.

Mare graben widths are used to estimate the minimum depth to a mechanical discontinuity (assumed to be the base of the regolith or possibly a basalt flow unit). Layer thickness calculations for graben associated with contractional features range from ~4 to 48 m, values within the range from other methods of determining minimum regolith thickness. In contrast, widths of mare graben independent of contractional features yield much greater thickness estimates, suggesting these graben are not confined to a near-surface regolith layer and indicative of a different mode of origin. Additionally, spacing of graben not associated with contractional landforms is used to estimate maximum local mare unit thickness (which is composed of multiple thinner flows) of 190 m for Posidonius and 296 m for Vitello.

While small-scale graben are globally distributed, they are commonly found near lobate scarps and wrinkle ridges. Some graben can be related to localized tension from flexural bending or dilation associated with lobate scarp and wrinkle ridge formation. Graben that do not match these criteria are difficult to associate with compressional tectonics, and other factors such as scale, morphology (including pit crater chains), and location along a topographic rise suggest influence from some other mechanism, perhaps volcanic uplift associated with a laccolith or dike intrusion. This hypothesis is consistent with evidence of young (<100 Ma) extrusive volcanism (Braden et al., 2014). Results presented in this paper are in agreement with Watters et al. (2012a): small-scale graben are young (maximum age of late Eratosthenian to early Copernican) and reflect localized extension either related to recent activity from contractional tectonics or uplift from intrusive volcanism. Additionally, their quantity and global distribution indicate a level of recent tectonic activity not previously recognized.

Acknowledgments

This work was supported by the NASA Lunar Reconnaissance Orbiter project and the Department of Earth and Planetary Sciences at Northwestern University. The authors would like to thank the LROC team for their hard work in data acquisition, distribution, and support, as well as the groups at Arizona State University and University of Arizona for processing NAC stereo pairs into digital elevation models. The authors would like to thank Brett Denevi for her thoughtful and constructive comments.

References

Ackermann, R.V., Schlische, R.W., 1997. Anticlustering of small normal faults around larger faults. Geology 25, 1127–1130.
Ackermann, R.V., Schlische, R.W., Withjack, M.O., 2001. The geometric and statistical evolution of normal fault systems: An experimental study of the effects of mechanical layer thickness on scaling laws. J. Struct. Geol. 23, 1803–1819.
Anderson, J.A. et al., 2004. Modernization of the integrated software for imagers and spectrometers. Lunar Planet. Sci. XXXV. Abstract #2039.
Arthur, D.W.G., 1962. Some systematic visual lunar observations. In: Kopal, Z., Mikhailov, Z.K. (Eds.), The Moon. Academies Press, London, pp. 317–324.
Bai, T., Pollard, D.D., 2000. Fracture spacing in layered rocks: A new explanation based on the stress transition. J. Struct. Geol. 22, 43–57.
Banerdt, W.B., Golombek, M.P., Tanaka, K.L., 1992. Stress and tectonics on Mars. In: Kieffer, H.H., Jakosky, B.M., Snyder, C.W., Matthews, M.S. (Eds.), Mars. University of Arizona Press, Tucson, AZ, pp. 249–297.
Banks, M.E. et al., 2012. Morphometric analysis of small-scale lobate scarps on the Moon using data from the Lunar Reconnaissance Orbiter. J. Geophys. Res. 117, E00H11.
Binder, A.B., Gunga, H.-C., 1985. Young thrust-fault scarps in the highlands: Evidence for an initially totally molten Moon. Icarus 63, 421–441.
Bonafede, M., Rivalta, E., 1999. The tensile dislocation problem in a layered elastic medium. Geophys. J. Int. 136, 341–356.
Braden, S.E. et al., 2014.. Evidence for basaltic volcanism on the Moon within the past 100 million years. Nat. Geosci. (advanced online publication).
Brennan, W.J., 1975. Modification of premare impact craters by volcanism and tectonism. The Moon 12, 449–461.
Buck, W.R., 1988. Flexural rotation of normal faults. Tectonics 7, 959–973.
Bürgmann, R., Pollard, D.D., Martel, S.J., 1994. Slip distributions on faults: Effects of stress gradients, inelastic deformation, heterogeneous host-rock stiffness, and fault interaction. J. Struct. Geol. 16, 1675–1690.
Cailleau, B. et al., 2003. Modeling volcanic deformation in a regional stress field: Implications for the formation of graben structures on Alba Patera, Mars. J. Geophys. Res. 108, 5141.
Campbell, N.P., Bentley, R.D., 1981. Late Quaternary deformation of the Toppenish Ridge uplift in south-central Washington. Geology 9, 519–524.
Cintala, M.J., McBride, K.M., 1995. Block distributions on the lunar surface: A comparison between measurements obtained from surface and orbital photography. NASA Technical Memorandum 104804.
Cowie, P.A., Roberts, G.P., 2001. Constraining slip rates and spacings for active normal faults. J. Struct. Geol. 23, 1901–1915.
Enns, A.C., Robinson, M.S., 2013. Basaltic layers exposed in lunar mare craters. Lunar Planet. Sci. XLIV. Abstract #2751.
Ernst, R.E. et al., 2003. Graben–fissure systems in Guinevere Planitia and Beta Regio (264–312°E, 24–60°N), Venus, and implications for regional stratigraphy and mantle plumes. Icarus 164, 282–316.
Freed, A.M. et al., 2012. On the origin of graben and ridges within and near volcanically buried craters and basins in Mercury's northern plains. J. Geophys. Res. 117, E00L06.
Gilbert, G.K., 1893. The Moon's face: A study of the origin of its features. Philos. Soc. Washington Bull. 12, 241–292.
Golombek, M.P., 1979. Structural analysis of lunar grabens and the shallow crustal structure of the Moon. J. Geophys. Res. 84, 4657–4666.
Golombek, M.P., Phillips, R.J., 2010. Mars tectonics. In: Watters, T.R., Schultz, R.A. (Eds.), Planetary Tectonics. Cambridge University Press, Cambridge, UK, pp. 183–232.
Gordon, F.R., Lewis, J.D., 1980. The Meckering and Caligiri earthquakes October 1986 and March 1970. Geological Survey of Western Australia Bulletin 126. 229p.

Grindrod, P.M. et al., 2005. Strain at radially fractured centers on Venus. J. Geophys. Res. 110, E12002.
Hansen, V.L., Phillips, R.J., 1993. Tectonics and volcanism of Eastern Aphrodite Terra, Venus: No subduction, no spreading. Science 260, 526–530.
Head, J.W. et al., 2009. Evidence for intrusive activity on Mercury from the first MESSENGER flyby. Earth Planet. Sci. Lett. 285, 251–262.
Howard, K.A., Muehlberger, W.R., 1973. Lunar thrust faults in the Taurus-Littrow region. Apollo 17 Preliminary Science Report, SP-330, pp. 31-22–31-25.
Jozwiak, L.M. et al., 2012. Lunar floor-fractured craters: Classification, distribution, origin and implications for magmatism and shallow crustal structure. J. Geophys. Res. 117, E11005.
Kennedy, P.J., Freed, A.M., Solomon, S.C., 2008. Mechanisms of faulting in and around Caloris basin, Mercury. J. Geophys. Res. 113, E08004.
Krassilnikov, A.S., Head, J.W., 2003. Novae on Venus: Geology, classification, and evolution. J. Geophys. Res. 108, 5108.
Losiak, A. et al., 2009. Lunar Impact Crater Database, Revised by Ohman (2011). Lunar and Planetary Institute, Houston, TX.
Maxwell, T.A., El-Baz, F., Ward, S.H., 1975. Distribution, morphology, and origin of ridges and arches in Mare Serenitatis. Geol. Soc. Am. Bull. 86, 1273–1278.
McGill, G.E., Stromquist, A.W., 1979. The grabens of Canyonlands National Park, Utah: Geometry, mechanics, and kinematics. J. Geophys. Res. 84, 4547–4563.
Mège, D., Cook, A.C., Garel, E., Lagabrielle, Y., Cormier, M.-H., 2003. Volcanic rifting at martian grabens. J. Geophys. Res. 108, 5044.
Melosh, H.J., McKinnon, W.B., 1988. The tectonics of Mercury. In: Vilas, F., Chapman, C.R., Matthews, M.S. (Eds.), Mercury. University of Arizona Press, Tucson, AZ, pp. 374–400.
Melosh, H.J., Williams Jr., C.A., 1989. Mechanics of graben formation in crustal rocks: A finite element analysis. J. Geophys. Res. 94, 13961–13973.
Philip, H., Meghraoui, M., 1983. Structural analysis and interpretation of the surface deformations of the El Asnam Earthquake of October 10, 1980. Tectonics 2, 17–49.
Phillips, R.J., Hansen, V.L., 1994. Tectonic and magmatic evolution of Venus. Annu. Rev. Earth Planet. Sci. 22, 597–654.
Pike, R.J., 1974. Ejecta from large craters on the Moon: Comments on the geometric model of McGetchin et al. Earth Planet. Sci. Lett. 23, 265–274.
Prockter, L.M. et al., 2010. Evidence for young volcanism on Mercury from the third MESSENGER flyby. Science 329, 668–671.
Quaide, W.L., Oberbeck, V.R., 1968. Thickness determinations of the lunar surface layer from lunar impact craters. J. Geophys. Res. 73, 5247–5270.
Robinson, M.S. et al., 2010. Lunar Reconnaissance Orbiter Camera (LROC) instrument overview. Space Sci. Rev. 150, 81–124.
Robinson, M.S. et al., 2012. Confirmation of sublunarean voids and thin layering in mare deposits. Planet. Space Sci. 69, 18–27.
Rubin, A.M., Pollard, D.D., 1988. Dike-induced faulting in rift zones of Iceland and Afar. Geology 16, 413–417.
Schlische, R.W. et al., 1996. Geometry and scaling relations of a population of very small rift-related normal faults. Geology 24, 683–686.
Scholten, F. et al., 2012. GLD100: The near-global lunar 100 m raster DTM from LROC WAC stereo image data. J. Geophys. Res. 117, E00H17.
Schultz, P.H., 1976. Floor-fractured lunar craters. Earth Moon Planets 15, 241–273.
Schultz, R.A. et al., 2004. Igneous dikes on Mars revealed by Mars Orbiter Laser Altimeter topography. Geology 32, 889–892.
Schultz, P.H., Staid, M.I., Pieters, C.M., 2006. Lunar activity from recent gas release. Nature 444, 184–186.
Schultz, R.A. et al., 2007. The Canyonlands model for planetary grabens: Revised physical basis and implications. In: Chapman, M. (Ed.), The Geology of Mars: Evidence from Earth-Based Analogs. Cambridge University Press, pp. 371–399.
Schultz, R.A. et al., 2010. Interpretation and analysis of planetary structures. J. Struct. Geol. 32, 855–875.
Schultz-Ela, D.D., Walsh, P., 2002. Modeling of grabens extending above evaporites in Canyonlands National Park, Utah. J. Struct. Geol. 24, 247–275.
Shearer, C.K. et al., 2006. Thermal and magmatic evolution of the Moon. In: Jolliff, B.L., Wieczorek, M.A., Shearer, C.K., Neal, C.R. (Eds.), New Views of the Moon. Reviews in Mineralogy & Geochemistry 60, pp. 365–518.
Shoemaker, E.M. et al., 1969. Observations of the lunar regolith and the Earth from the television camera on Surveyor 7. J. Geophys. Res. 74, 6081–6119.
Smith, D.E. et al., 2010. Initial observations from the Lunar Orbiter Laser Altimeter (LOLA). Geophys. Res. Lett. 37, L18204.
Soliva, R., Benedicto, A., 2005. Geometry, scaling relations and spacing of vertically restricted normal faults. J. Struct. Geol. 27, 317–325.
Soliva, R., Benedicto, A., Maerten, L., 2006. Spacing and linkage of confined normal faults: Importance of mechanical thickness. J. Geophys. Res. 111, B01402.
Solomon, S.C., 1977. The relationship between crustal tectonics and internal evolution in the Moon and Mercury. Phys. Earth Planet. Inter. 15, 135–145.
Solomon, S.C. et al., 1991. Venus tectonics: Initial analysis from Magellan. Science 252, 297–312.
Speyerer, E.J., Robinson, M.S., Denevi, B.W., and LROC Science Team, 2011. Lunar Reconnaissance Orbiter Camera global morphological map of the Moon. Lunar Planet. Sci. XLII. Abstract #2387.
Stöffler, D., Ryder, G., 2001. Stratigraphy and isotope ages of lunar geologic units: Chronological standard for the inner Solar System. Space Sci. Rev. 96, 9–54.
Trask, N.J., 1971. Geologic Comparison of Mare Materials in the Lunar Equatorial Belt, Including Apollo 11 and Apollo 12 Landing Sites. Geological Survey Professional Paper 750-D, D138–D144.
Watkins, J.S., Kovach, R.L., 1972. Apollo 14 seismic experiment. Science 175, 1244–1245.
Watters, T.R., Johnson, C.L., 2010. Lunar tectonics. In: Watters, T.R., Schultz, R.A. (Eds.), Planetary Tectonics. Cambridge University Press, Cambridge, UK, pp. 121–182.
Watters, T.R., Schultz, R.A., 2010. Planetary tectonics. Cambridge University Press, New York.
Watters, T.R., Nimmo, F., Robinson, M.S., 2005. Extensional troughs in the Caloris basin of Mercury: Evidence of lateral crustal flow. Geology 33, 669–672.
Watters, T.R. et al., 2009. Emplacement and tectonic deformation of smooth plains in the Caloris basin, Mercury. Earth Planet. Sci. Lett. 285, 309–319.
Watters, T.R. et al., 2010. Evidence of recent thrust faulting on the Moon revealed by the Lunar Reconnaissance Orbiter Camera. Science 329, 936–940.
Watters, T.R. et al., 2012a. Recent extensional tectonics on the Moon revealed by the Lunar Reconnaissance Orbiter Camera. Nat. Geosci. 5, 181–185.
Watters, T.R. et al., 2012b. Extension and contraction within volcanically buried impact craters and basins on Mercury. Geology 40, 1123–1126.
Wichman, R.W., Schultz, P.H., 1995. Floor-fractured craters in Mare Smythii and west of Oceanus Procellarum: Implications of crater modification by viscous relaxation and igneous intrusion models. J. Geophys. Res. 100, 21201–21218.
Wichman, R.W., Schultz, P.H., 1996. Crater-centered laccoliths on the Moon: Modeling intrusion depth and magmatic pressure at the crater Taruntius. Icarus 122, 193–199.
Wilcox, B.B. et al., 2005. Constraints on the depth and variability of the lunar regolith. Meteorit. Planet. Sci. 40, 695–710.
Wilhelms, D.E., 1987. The Geologic History of the Moon. USGS Professional Paper 1348.
Wilson, L., Head, J.W., 2002. Tharsis-radial graben systems as the surface manifestation of plume-related dike intrusion complexes: Models and implications. J. Geophys. Res. 107, 1–24.
Wyrick, D. et al., 2004. Distribution, morphology, and origins of martian pit crater chains. J. Geophys. Res. 109, E0600.